EXPERIMENTAL AND NUMERICAL INVESTIGATIONS ON COLD-FORMED STEEL BEAMS ASSEMBLED BY MIG BRAZING

Ioan BOTH[1]; Viorel UNGUREANU[1]; Daniel TUNEA[1]; Andrei CRIŞAN[1]; Marius GROŞAN[1]
[1] Politehnica Univesity of Timişoara, Romania

ABSTRACT

The efficient joining of cold-formed steel elements is a major concern for lightweight structural systems especially when a built-up element is in the discussion. The developments in the welding techniques made several solutions to be highly attractive, among them spot welding and MIG brazing. The WELLFORMED research project, ongoing at the CEMSIG Research Center of the Politehnica University of Timisoara, proposes to study built-up beams made of corrugated steel sheets for the web and thin-walled cold-formed steel profiles for the flanges using these welding solutions. The paper presents the research performed on such built-up beams using MIG brazing as connecting technique, while the research on similar beams using spot welding was already presented in an accompanying paper. The research started with the investigations on lap joints specimens, material testing and full-scale testing of beams, highlighting the advantages and disadvantages of the proposed solutions. A numerical model is calibrated and validated based on the experimental results.

Keywords: Built-up beams; Corrugated web; MIG Brazing; Experimental tests; Numerical analysis

1. INTRODUCTION

Built-up beams made of cold-formed steel elements represent an attractive solution due to their efficient use of material and their standardized design according to EN 1993 [1-3].

The technical solution of corrugated web beams with parallel flanges made of thin-walled cold-formed steel lipped channel profiles connected using spot welding was already studied within the WELLFORMED research project and presented in [4]. In order to evaluate the response of such beams using other types of connection between the beam components, the MIG brazing is considered for the current study.

The spot welding technique for connecting the components of built-up beams was presented in [4], and the results showed an increased stiffness and decreased ductility with failures caused by both the distortions of the web corrugations and the spot welding failure after reaching maximum force when compared to the self-drilling screws solution [5,6].

The new proposed solution for the built-up beams is based on an arc brazing process with lower heat input, with filler material and with inert gas shielding, MIG brazing. Although the brazing represents a joining process for a vast variety of materials, light-gauge steel sheets present a particularity due to the corrosive protection in the shape of the zinc coating. Due to the vaporization of zinc, at around 906 °C, the welding may show pores, cracking and unsteady arc, making the use of bronze welding wires more suitable [7]. By this technique, the level of corrosion protection is close to its original value. The brazing concept is not new but the developments of the filler material by copper alloys made this technique more attractive [8].

A detailed overview of the joining of different sheets by Cold Metal Transfer (CMT), a process that is contained in the MIG welding category, is presented in [9], in relation to its applications in the industry. Studies on the process parameters and shielding gases influences in MIG brazed joints of the thin zinc coated steel plates were performed in [10] listing the adequate gases to be used, heat input and welding speed to be set for a good stability of the welding. Similar investigations on aluminum alloys were also presented in [11].

Also, of high interest is MIG welding-brazing process for aluminium alloys and stainless

[1] viorel.ungureanu@upt.ro (corresponding author), ioan.both@upt.ro, mircea.burca@upt.ro, andrei.crisan@upt.ro, gmbmaryus@yahoo.com

steels but an accurate parameter setting for the weld is necessary for a good joint [12].

Recent studies are directed either towards the welding of high strength steels [13] where microstructure changes are affecting the mechanical properties or towards the welding of dissimilar metals [14] where the joint may become brittle.

The Cold Metal Transfer is in continuous progress as the improvements presented in [15] are proving, by the addition of pulses to the conventional welding process, the performance of the technique.

The paper presents the results of the experimental program performed on lap joint specimens subjected to tension, base material tensile tests and full-scale tests on built-up beams of corrugated web and cold-formed steel elements as flanges connected by MIG brazing.

2. EXPERIMENTAL INVESTIGATIONS

A research on the new connecting solution to be used for built-up cold-formed steel beams with the cross-section made of corrugated steel webs and flanges made of thin-walled cold-formed steel profiles, i.e. MIG brazing, is in progress within the CEMSIG Research Center (http://www.ct.upt.ro/en/centre/cemsig) of the Politehnica University of Timisoara under the WELLFORMED research project. The research project involves a large experimental program on lap joint specimens subjected to tension, material tests and tests on full-scale beams, to assess the response of the proposed solution followed by numerical simulations to optimize the connecting technique and to extend the solution applicability by parametric numerical studies.

The proposed solution enlarges the database and knowledge on the built-up beams using cold-formed steel components previously developed within the CEMSIG Research Center, in which five corrugated web beams with flanges of back-to-back cold-formed lipped channel steel profiles were tested, having a span of 5157 mm and a height of 600 mm, with different arrangements/configurations for the self-drilling screws position and for shear panels as presented in [5,6] as well as for beams connected using spot welding [4].

The joining of thin steel sheets by MIG brazing requires a welding technique which induces a lower thermal input in order to avoid the melting of the base material but still melting the filler material. An improved equipment based on electric pulses produced by REHM GmbH, MEGAPULS.FOCUS 330, was used for the brazing process. The filler material was CuAl 8 according to EN 14640 [16], wire with 1 mm diameter.

The experimental results consist of tensile tests on lap joint specimens with various thickness combinations, tensile tests on the base material and tests on three full-scale built-up beams

2.1 The lap joint specimens

As the full-scale built-up beams consist of joining various thinner sheets of the web to the thicker flanges or shear panels, lap joint specimens were tested to assess their response to mechanical loading.

Seven specimens having a width of 50 mm, as shown in Figure 1, and welded with two beads, were tested for each combination of sheets thicknesses as presented in Table 1. Similar specimens were tested in [4] but using spot welding.

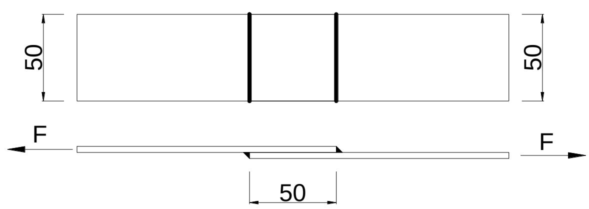

Figure 1: The dimensions of the lap joint specimens

The experimental tests were conducted on a UTS universal testing machine where the load was monitored by the machine load cell and the elongation was monitored by the Zwick contact extensometer. The distance between the sensors of the extensometer was set to 80 mm.

Table 1: Types of lap joint specimens

Name	No. of tests	Nominal dimensions			Measured dimensions		Failure mode
		t_1 [mm]	t_2 [mm]	b_{nom} [mm]	min(t) [mm]	$b_{measured}$ [mm]	
CMT-0.8-0.8	7	0.80	0.80	50	0.79	49.76	Heat affected zone
CMT-0.8-1.0	7	0.80	1.00	50	0.79	49.76	Heat affected zone
CMT-0.8-1.2	7	0.80	1.20	50	0.80	49.78	Heat affected zone
CMT-0.8-1.5	7	0.80	1.50	50	0.81	49.77	Heat affected zone
CMT-0.8-2.0	7	0.80	2.00	50	0.81	49.67	Heat affected zone
CMT-0.8-2.5	7	0.80	2.50	50	0.82	49.82	Heat affected zone
CMT-1.0-1.0	7	1.00	1.00	50	1.02	49.16	Heat affected zone
CMT-1.0-1.2	7	1.00	1.20	50	1.00	49.84	Heat affected zone
CMT-1.0-1.5	7	1.00	1.50	50	0.99	49.94	Heat affected zone
CMT-1.0-2.0	7	1.00	2.00	50	1.00	49.64	Heat affected zone
CMT-1.0-2.0	7	1.00	2.50	50	1.00	50.06	Heat affected zone
CMT-1.2-1.2	7	1.20	1.20	50	1.19	49.56	Heat affected zone
CMT-1.2-1.5	7	1.20	1.50	50	1.20	49.59	Heat affected zone
CMT-1.2-2.0	7	1.20	2.00	50	1.20	49.84	Heat affected zone
CMT-1.2-2.5	7	1.20	2.50	50	1.21	49.82	Heat affected zone
CMT-1.5-1.5	7	1.50	1.50	50	1.50	49.77	Heat affected zone
CMT-1.5-2.0	7	1.50	2.00	50	1.49	49.76	Heat affected zone
CMT-1.5-2.5	7	1.50	2.50	50	1.50	49.72	Heat affected zone
CMT-2.0-2.0	7	2.00	2.00	50	2.00	49.99	Heat affected zone
CMT-2.0-2.5	7	2.00	2.50	50	1.93	50.02	Heat affected zone

The performed tests revealed the two failure modes, i.e. fracture of the material close to the weld, in the heat affected zone, as shown in Figure 2(a), and base material fracture (see Figure 2(b)). The second type of failure was seldom encountered, most of the failures being categorized as fracture of the material close to the weld in the heat affected zone. The measured dimensions and failure modes are presented in Table 2.

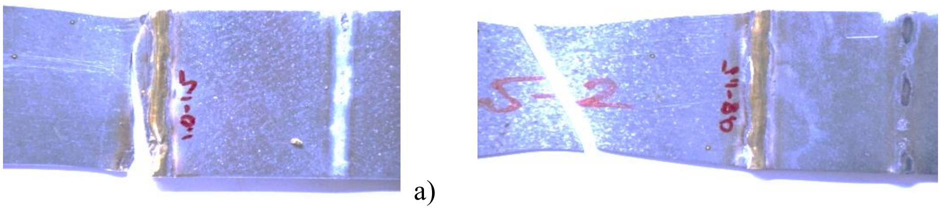

a) b)

Figure 2: Failure modes of the lap joint specimens: a) fracture in the heat affected zone; b) base material fracture

Although not all specimens failed by base material fracture, it can be seen the MIG brazing possesses a very good resistance.

Since similar steel sheets were used in the solution of the built-up beams using spot welding, the results tensile tests on the base material presented in [4], are valid for the current solution where the Cold Metal Transfer is used.

2.2 Full-scale beam specimen tests

For the full-scale specimen tests, three beams were built-up, namely CWB-CMT1, CWB-CMT2 and CWB-CMT3, having a span of 5157 mm and a height of 600 mm. The process for the manufacturing consists of 4 steps: 1) connecting the corrugated steel sheets for the web, 2) connecting the shear panels at the ends of the beam, 3) connecting the top and bottom flanges and 4) connecting the end parts of the beam for the rigid connection to the experimental stand. The first step is only necessary if the corrugated web is not available in one piece. For the current case, the corrugated sheets had a maximum length of 1.05 m and, for a precise initial positioning of the web, the corrugated parts were connected by spot welding.

The components of the built-up beams are shown in Figure 3 and are detailed below:

- two back-to-back lipped channel sections for flanges - 2×C120/2.0;
- corrugated steel sheets (panels of 1.05 m length with 0.8, 1.0 and 1.2 mm thicknesses);
- additional shear panels - flat plates of 1.0 or 1.2 mm;
- reinforcing profiles U150/2.0 used under the load application points;
- bolts M12 grade 8.8 for the flange to endplate connection.

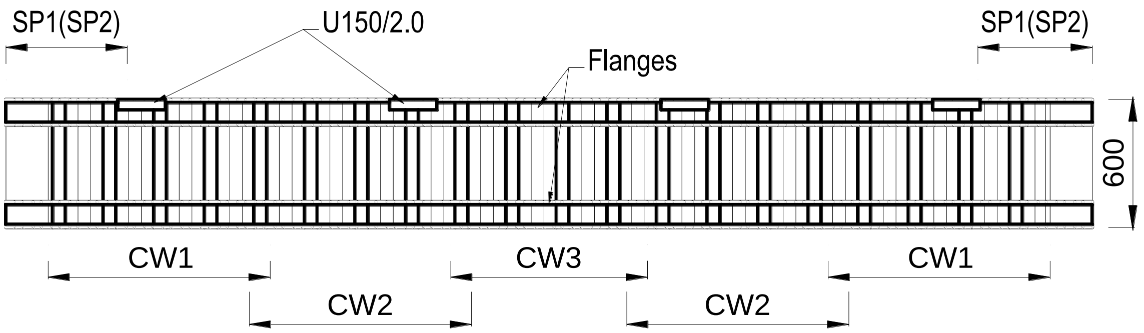

Figure 3: Components of the built-up beams

The position of the MIG brazing is similar for all three specimens (see Figure 4(a)), the difference regards only the thickness of the corrugated web and the shear panel thickness as presented in Table 2.

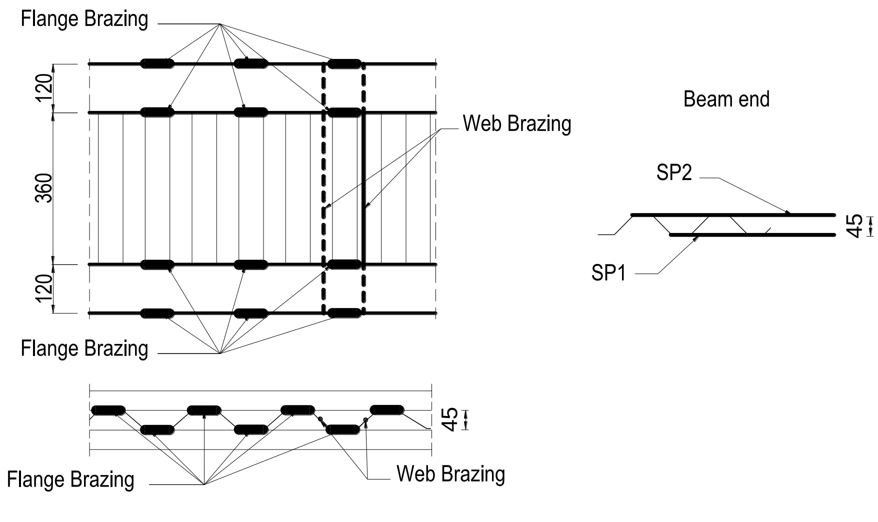

Figure 4: a) Position of the brazing on the corrugated web beam, b) position of the shear panel

Table 2: Characteristics of the steel sheets used for the beams using MIG brazing

Name	Thickness				Length of shear panels*
	CW1	CW2	CW3	SP1 (SP2)	
CWB-CMT1	1.2 mm	0.8 mm	0.8 mm	1.2 mm	470 mm; 570 mm
CWB-CMT2	0.8 mm	0.8 mm	0.8 mm	1.0 mm	470 mm; 570 mm
CWB-CMT3	1.0 mm	0.8 mm	0.8 mm	1.0 mm	470 mm; 570 mm

* the length of the shear panels is different due to variable position of the web corrugation (see Figure 4(b))

Finally, the beams with the configuration presented above were loaded in a 2D loading frame, with the test set-up depicted in Figure 5. The beam was loaded by an actuator of 500 kN which transmitted the force to the beam by a mechanism able to distribute the load in 4 points. An out-of-plane independent frame was used to avoid stability problems during loading.

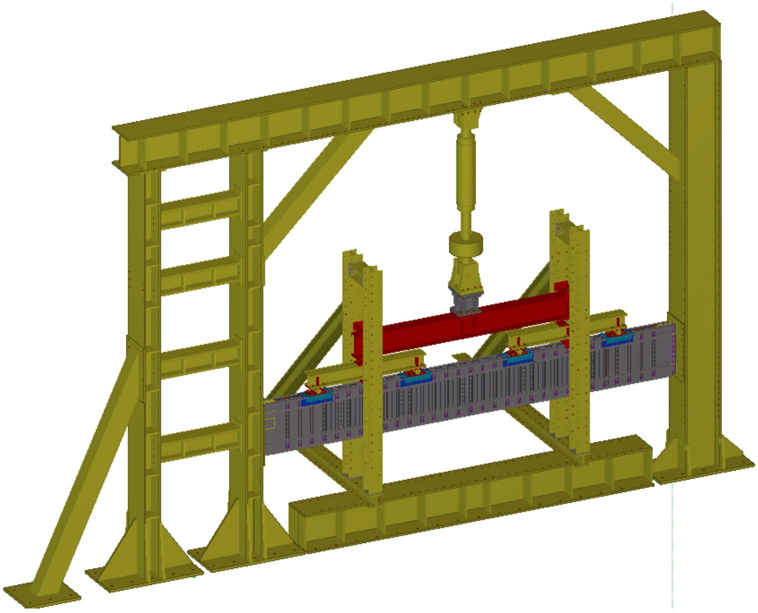

Figure 5: Test setup of the full-scale beams

The recordings aimed to monitor the displacements at each end of the top and bottom flange, between the flange and the end plate as well as between the end plate and the rigid frame. The deflection of the beam was monitored at each quarter of the span by 2 wire displacement transducers connected to each of the bottom flange parts, as presented in. The force was recorded through the actuators load cell.

3. RESULTS AND DISCUSSIONS

Due to the initial imperfections caused by the MIG brazing process on the lap joint specimens, the results may not be assessed by their initial stiffness. In terms of resistance, the lap joint specimens maximum force is very close to the maximum force of the base materials (see Figure 6).

Also, contrary to the simple specimens tested in [4] by using spot welding, the maximum resistance of the MIG brazed specimens show similar values for the same set of specimens, meaning that the resistance of the combinations of different sheet thicknesses is the same with the minimum thickness sheet of the lap joint specimen. It may be noticed that, except to the 1.5-2.5 mm combination specimens, the response of the lap joint specimens is a smooth ductile behaviour, with no fragile breakage of the connection.

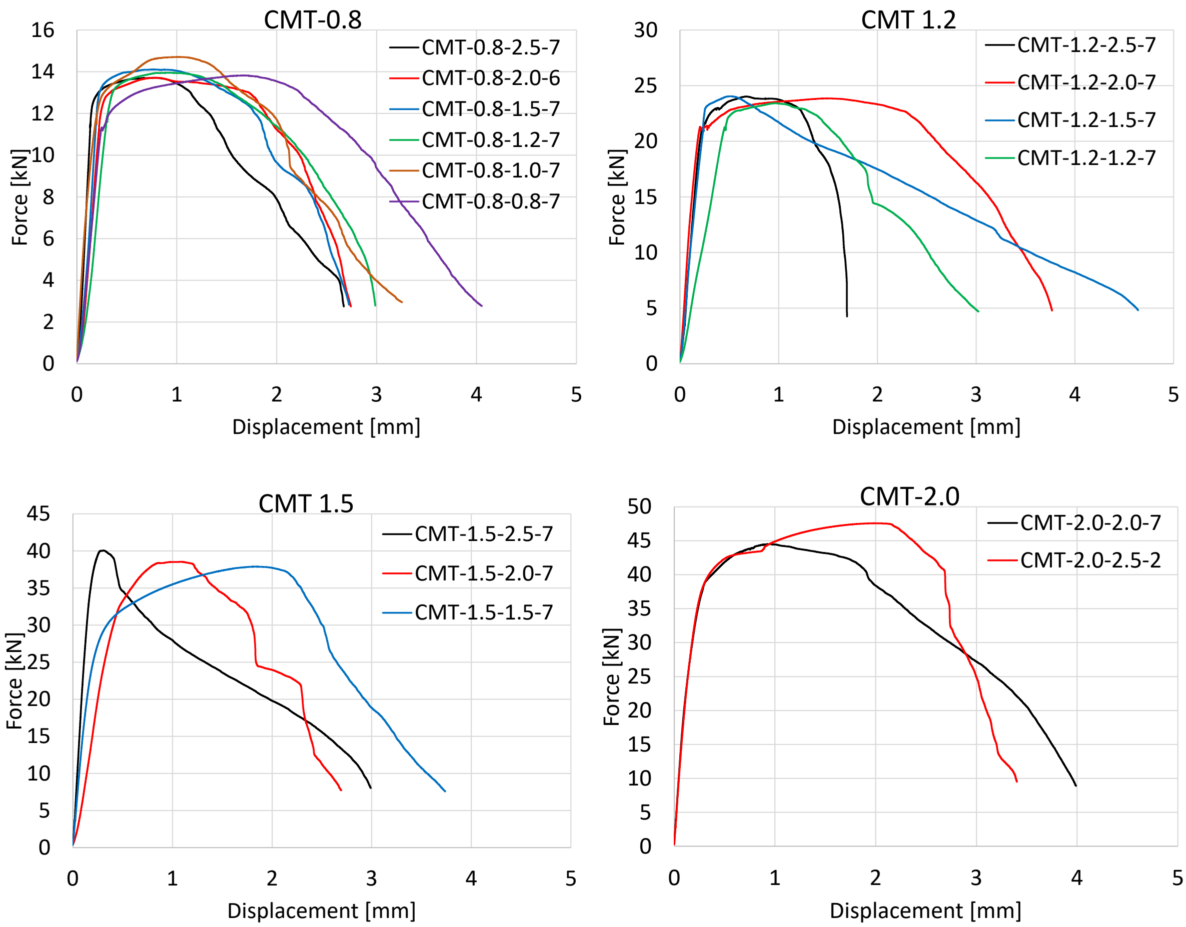

Figure 6: Response of simple brazed specimens

For the first tested specimen, CWB-CMT1, presented in Figure 7, the failure mode of the beam started with the buckling of the shear panel as shown in Figure 8(a), followed by the shear buckling of the corrugations of the web (see Figure 8(b)), and finally the shear buckling of the web plates and local buckling of the flanges, under the load application points, as presented in Figure 8(c). The behaviour of CWB-CMT1 beam was ductile and the maximum load is reached at F_{max} = 368.2 kN (the initial stiffness of $K_{0\text{-}Exp}$ was not possible to be determined). The collapse appears for a displacement of 96.6 mm.

Figure 7: Deformed shape of CWB-CMT1

a) b) c)

Figure 8: Failure stages for CWB-CMT1: a) shear panels buckling; b) corrugations shear buckling; c) web shear buckling and flange local buckling

The second beam, CWB-CMT2 (see Figure 9) presented a similar mechanism of the failure mode starting with the buckling of the shear panel (Figure 10(a)), followed by the shear buckling of the corrugations (Figure 10(b)), and finally, the shear buckling of the web sheets (Figure 10(c)). The behaviour was ductile, with an initial stiffness of $K_{0\text{-}Exp}$ = 22559 N/mm and the maximum capacity is achieved at F_{max} = 227.9 kN.

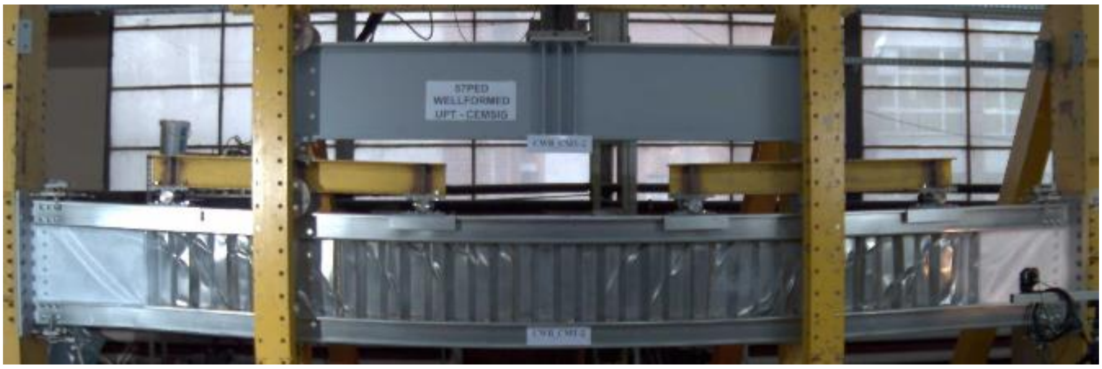

Figure 9: Deformed shape of CWB-CMT2

a) b) c)

Figure 10 Failure stages for CWB-CMT2: a) shear panels buckling; b) corrugations distortions; c) web plates shear buckling

An optical monitoring system was used in order to assess the behaviour of the shear panels during the loading. The shear panels were monitored using a digital image correlation system (DIC) provided by isi-sys GmbH. Two GT6600 Prosilica series of high-resolution cameras (29

Mpix) with 35 mm lenses, recorded images for a 3D evaluation of the out of plane displacements and strain of the shear panel, at an acquisition frequency of 1 Hz.

A facet size (number of pixels per subset) and a step size (the spacing of the points that are analysed during correlation) of 10×10 and 5, respectively, were considered for an initial processing.

Figure 11 depicts the evolution during testing of the out of plane deformations (a, b, c) and the corresponding principal strains (d, e, f) of a monitored shear panel.

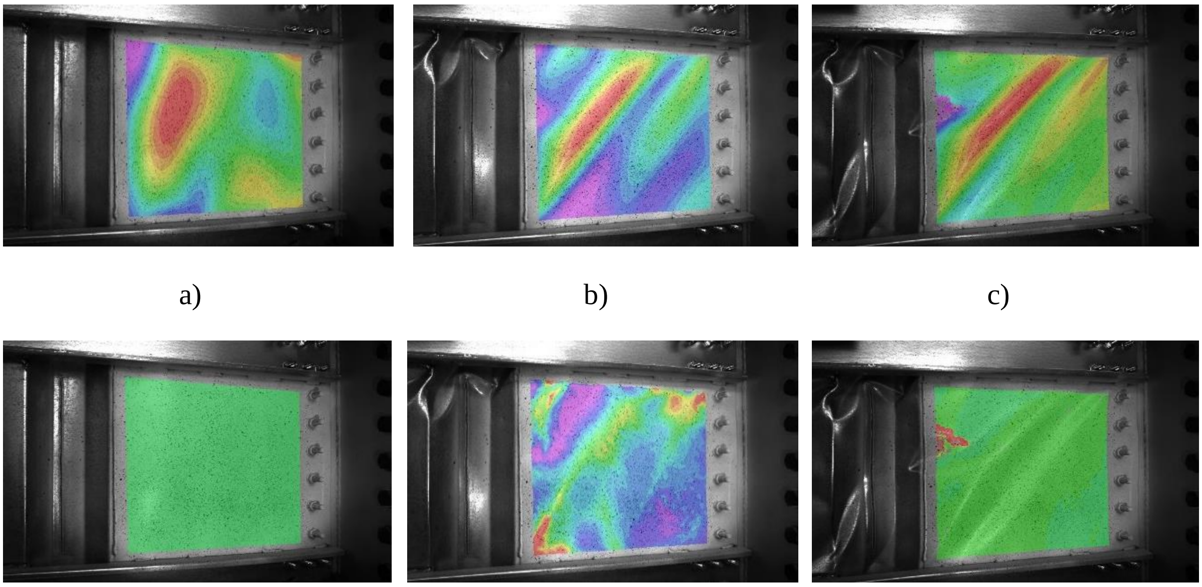

a) b) c)

d) e) f)

Figure 11: Evolution of the out of plane deformations (a, b, c) and the corresponding principal strains (d, e, f) of a given shear panel

Although the strains at the beginning of the tests are null, the out-of-plane images recorded imperfections due to fabrication up to 11 mm. In the final stage of the loading, after the buckling, the shear panel exhibited a local distortion where substantial strains were concentrated.

The third beam (see Figure 12), CWB-CMT3, presented a similar mechanism of the failure mode starting with the buckling of the shear panels, presented in Figure 13(a), followed by the shear buckling of the corrugations, Figure 13(b), and, finally, the web plates shear buckling, Figure 13(c). The behaviour was ductile, with an initial stiffness of $K_{0\text{-}Exp}$ = 24792 N/mm and the maximum capacity is achieved at F_{max} = 273.5 kN.

Figure 12: Deformed shape of CWB-CMT3

a) b) c)

Figure 13: Failure stages of CWB-CMT3: a) shear panels buckling; b) corrugations shear buckling; c) web plates shear buckling

The force-displacement curves are depicted in Figure 14 and Table 3 where it is observed that the higher capacity corresponds to the combination of higher thicknesses of the shear panels and corrugated web panels of the specimens.

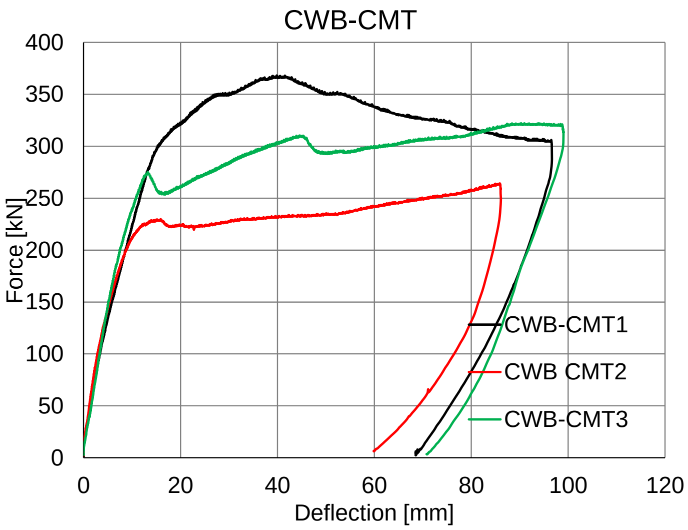

Figure 14: Force-displacement curves for the full-scale built-up beams

Table 3: Results of the corrugated web beams with MIG brazing

Beam type	$K_{0\text{-}Exp}$ (N/mm)	$F_{max\text{-}Exp}$ (kN)
CWB-CMT1	N/A	368.2
CWB-CMT2	22559	227.9
CWB-CMT3	24792	273.5

4. Numerical analyses

A series of finite element analysis (FEA) numerical models were created to extend the numerical database. For this, Abaqus v. 6.14 [17] was used to define/model/analyse the cold-formed beams.

Since cold-formed thin-walled elements were involved in the tests, shell elements were assumed for the simulations. S4R elements (doubly curved shell elements with 4 nodes and reduced integration) were used to simulate the behaviour of the beams. Since no weld failure was observed for the CMT welding specimens, the welding zones were modelled using a *Tie* constraint.

Due to a considerable number of contact areas and the increased associated computational demand, a *Dynamic/Explicit* model was assumed with an *All with self* contact approach.

A *Kinematic coupling* constraint was defined for the loading pads to model the load transferring system, as presented in the figure above. At the middle, the control point was assigned an imposed displacement (i.e. 80 mm) in the gravitational direction, to simulate the loading. All other degrees of freedom were assumed to be zero. To model the supports, all the corresponding nodes associated with the bolt holes were assumed to be fixed.

With the considered input data for the finite element model, the qualitative results are presented in Figure 15 as the deformed shape of the beams and stress distribution within the parts of the beam.

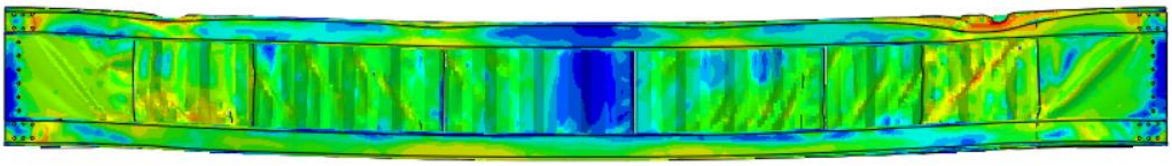

a)

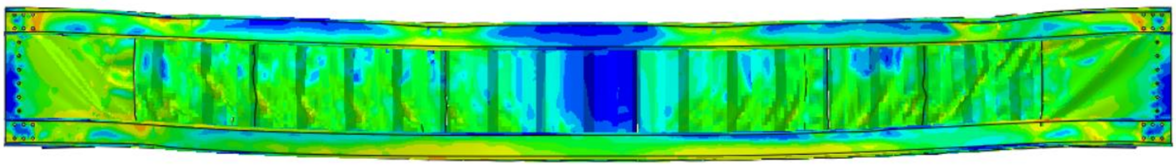

b)

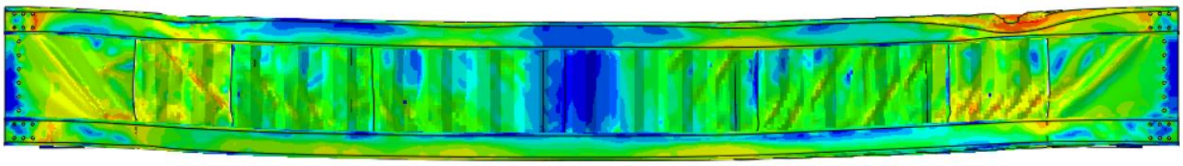

c)

Figure 15: Deformed shape and stress distribution for: a) CWB-CMT1, b) CWB-CMT2, c) CWB-CMT3

The numerical model closely replicates the response of the shear panels and the corrugated web. The shear buckling of the shear panels, the local buckling of the flanges as well as the web crippling of the corrugated steel sheets are depicted in Figure 16.

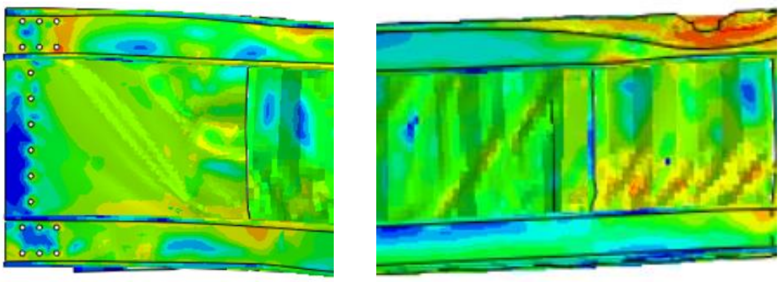

Figure 16: Instabilities developed by the beams

Also, the numerical model is able to acquire the quantitative results in terms of total force - midspan deflection as presented in Figure 17.

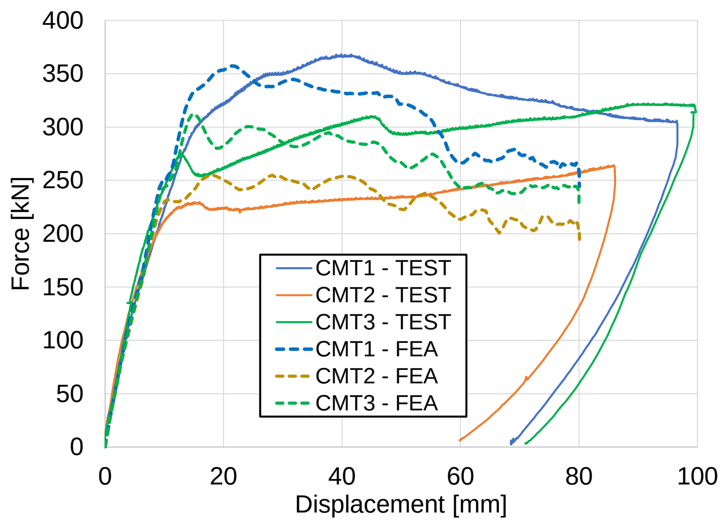

Figure 17: Comparison of the experimental and numerical results

From the figures above, it can be easily observed that the failure mechanism is related to the shear buckling of the support web panels. In the same time, the force-displacement curves confirm the influence of the shear panels strength (directly related to the thickness) onto the ultimate strength of the tested beams.

5. CONCLUSIONS

Within the WELLFORMED research project, carried out at the CEMSIG Research Center of the Politehnica University of Timisoara, an extensive experimental program on built-up cold-formed steel beams using MIG brazing as connecting technology was performed.

The paper presents the experimental results on tensile tests on lap joint specimens, in order to characterize the behaviour of these connections and on full-scale tests of three beams subjected to bending. The experiments were accompanied by tensile tests, to characterize the material behaviour.

Although base material fracture was also recorded, the most common failure mode for the tensile tests on lap joint brazed specimens was the fracture in the heat affected zone. Both the resistance and the ductility obtained for the tested specimens are very good and compared to the similar specimens tested using self-drilling screws [5,6], or the specimens connected by spot welding [4], the capacity is very much increased.

The experimental results of full-scale specimens shown:

- both the capacity and the ductility obtained for the tested specimens are very good;

- compared to the solution studied in [4], the results show an increased rigidity mainly due to the stabilizing effect of the brazing; a higher capacity may be attained but depends on the web thicknesses.

It is considered that the major advantage of the MIG brazing joints is the increased stability of the corrugations since no distortion of the web corrugations was recorded. A disadvantage of the current solution is the increased time for manufacturing compared to spot welding solution.

The results obtained from the numerical analysis, similarly catch the response of the experimental investigations on the real scale beams, both from qualitative and quantitative results.

By this calibration and validation of the numerical models, parametric studies will follow the evaluate the suitability of the corrugated web beams with cold-formed thin-walled elements, for larger spans.

6. ACKNOWLEDGEMENTS

This work was supported by a grant of the Romanian National Authority for Scientific Research and Innovation, CNCS/CCCDI-UEFISCDI, project number PN-III-P2-2.1-PED-2016-1684 / WELLFORMED - Fast welding cold-formed steel beams of corrugated sheet web, within PNCDI III.

REFERENCES

1. *EN 1993-1-5, Eurocode 3: Design of steel structures - Part 1-5: Plated structural elements*, CEN, Brussels, 2006.
2. *EN 1993-1-1, Eurocode 3: Design of steel structures - Part 1-1: General rules and rules for buildings*, CEN, Brussels, 2005.
3. *EN 1993-1-3, Eurocode 3: Design of steel structures. Part 1-3: General Rules. Supplementary rules for cold-formed thin gauge members and sheeting*, CEN, Brussels, 2006.
4. Ungureanu V., Both I., Burca M., Crisan A. and Grosan M., "Experimental and numerical investigations on cold-formed steel beams assembled by resistance spot welding", *International Conference on Engineering Research and Practice for Steel Construction 2018 (ICSC2018)*, Hong Kong, China, 2018 (in this volume).
5. Dubina D., Ungureanu V. and Gîlia L. (2015). "Experimental investigations of cold-formed steel beams of corrugated web and built-up section for flanges", *Thin-Walled Structures*, 90, 159-170.
6. Dubina D., Ungureanu V. and Gîlia L. (2013). "Cold-formed steel beams with corrugated web and discrete web-to-flange fasteners", Steel Construction, 6(2), 74-81.
7. Hackl H., MIG brazing of galvanised light-gauge sheets, www.fronius.com.
8. Milner D.R. and Apps R.L., *Introduction to Welding and Brazing*, Robert Maxwell MC MP Minnesota, 1969.
9. Selvi S., Vishvaksenan A. and Rajasekar E. (2018). "Cold metal transfer (CMT) technology - An overview", *Defence Technology*, 14, 28-44.
10. Iordachescu D., Quintino L., Miranda R. and Pimenta G. (2006). "Influence of shielding gases and process parameters on metal transfer and bead shape in MIG brazed joints of the thin zinc coated steel plates", *Materials & Design*, 27 (5), 381-390.
11. Kumar N.P., Vendan S.A. and Shanmugam N.S. (2016). "Investigations on the parametric effects of cold metal transfer process on the microstructural aspects in AA6061". *Journal of Alloys and Compounds*, 658, 255-264.
12. Zhang H., Liu J. and Feng J. (2014). "Effect of auxiliary TIG arc on formation and microstructures of aluminum alloy/stainless steel joints made by MIG welding-brazing process". *Transactions of Nonferrous Metals Society of China*, 24 (9), 2831-2838.
13. Shome M. (2015). "Metal inert gas (MIG) brazing and friction stir spot welding of advanced high-strength steels". *Welding and Joining of Advanced High Strength Steels (AHSS)*, Woodhead Publishing, 137-165, Waltham, USA, 2015.
14. Jing S., Kehong W., Qi Z., Deku Z., Jun H., Guangle L. (2013). "Microstructure Characteristics and Properties of Mg/Al Dissimilar Metals Made by Cold Metal Transfer Welding with ER4043 Filler Metal". *Rare Metal Materials and Engineering*, 42 (7), 1337-1341.
15. Pang J., Hua S., Shena J., Wang P. and Lianga Y. (2016). "Arc characteristics and metal transfer behavior of CMT + P welding process". *Journal of Materials Processing Technology*, 238, 212-217.
16. *EN 14640, Welding consumables. Solid wires and rods for fusion welding of copper and copper alloys*. Classification, CEN, Brussels, 2005.
17. *Dassault Systemes, Abaqus 6.14 Documentation*, Simulia Systems, Providence, RI, 2014.